15 Apr 2023

Experimental and Numerical Studies of Slurry-Based Coextrusion Deposition of Continuous Carbon Fiber Micro-Batteries to Additively Manufacture 3D Structural Battery Composites

Aditya R. Thakur

Xiangyang Dong
Missouri University of Science and Technology, dongxi@mst.edu

Recommended Citation

A. R. Thakur and X. Dong, "Experimental and Numerical Studies of Slurry-Based Coextrusion Deposition of Continuous Carbon Fiber Micro-Batteries to Additively Manufacture 3D Structural Battery Composites," *Composites Part B: Engineering*, vol. 255, article no. 110632, Elsevier, Apr 2023.
The definitive version is available at https://doi.org/10.1016/j.compositesb.2023.110632

Composites Part B 255 (2023) 110632

Contents lists available at ScienceDirect

Composites Part B

journal homepage: www.elsevier.com/locate/compositesb

Experimental and numerical studies of slurry-based coextrusion deposition of continuous carbon fiber micro-batteries to additively manufacture 3D structural battery composites

Aditya R. Thakur, Xiangyang Dong *

Mechanical and Aerospace Engineering, Missouri University of Science and Technology, Rolla, MO, USA

ARTICLE INFO

Handling Editor: Dr Uday Vaidya

Keywords:
Additive manufacturing
Structural battery composite
Multifunctional composite
Computational fluid dynamics analysis
Continuous carbon fiber

ABSTRACT

Carbon fiber structural battery composites have recently attracted growing interests due to their potentials of simultaneously carrying mechanical loads and storing electrical energy for lightweight application. In this study, we present a slurry-based coextrusion deposition method to additively manufacture 3D structural battery composites from carbon fiber micro-batteries. Cathode slurry is coextruded together with solid polymer electrolyte-coated carbon fibers in a single deposition. A network of carbon fiber micro-batteries is achieved within the fabricated structural battery composites. Electrochemical tests show a stable charge-discharge performance up to 100 cycles. The rheological behavior of the cathode slurry is found to govern the coextrusion process and the obtained electrochemical-mechanical properties. The rheological measurements are first used to identify printability windows in terms of solid loadings and binder contents in the cathode slurry. Increasing binder contents improve the mechanical properties, with maximum 1.1 GPa and 124 GPa obtained for tensile strength and modulus, respectively, but lowers the obtained electrochemical performance. Lowering solid loadings improves printability, simultaneously increasing electrochemical capacity (by 106%) and tensile modulus (by 108%) and strength (by 40%). Further microstructural characterization shows that residual voids play a major role in the obtained electrochemical and mechanical properties. A meso-scale computational fluid dynamics simulation is used to understand void formation during the coextrusion process. The cathode slurry rheology mainly affects degree of impregnation. The findings help understand the effects of the cathode slurry on 3D printing and how to further improve multifunctional performance for electrically powered structural systems where lightweight materials are in strong demands.

1. Introduction

The rapidly increasing demand in mobile electric technologies has necessitates the development of lightweight materials to promote operation range and service life for portable electronics and electric aircraft and vehicles. A key challenge is to develop energy storage systems with high gravimetric and volumetric efficiency, which directly determines the operation range of electric transportation. One disruptive approach is to reduce system mass and volume and promote system-level performance and efficiency by integrating functions of electrical energy storage and load bearings into a single material (e.g., structural battery composite). Structural battery composite addresses the need to maximize energy storage and to simultaneously minimize size and weight by intrinsically storing electrical energy while being a part of the load carrying structure itself. Due to the potentials of such multifunctional composites, they are being investigated as multifunctional engineering materials for a diverse range of applications, e.g., structural energy storage [1], sensing [2], health monitoring [2], energy harvesting [3], and morphing [4].

Carbon fiber reinforced composites are widely used for lightweight high-strength structural applications. They have also recently been developed for structural battery composites that can simultaneously carry mechanical loads as a structural material and store electrical energy as a battery [5]. The achieved synergistic multifunctionality allows for significant mass and volume savings and increases specific energy storage at a system level [5] for electrically powered structural systems. In addition to electric vehicles [6], it can be transformative to the future of many systems, such as electric aircraft [7], spacecraft [8], and ships

* Corresponding author.
E-mail address: dongxi@mst.edu (X. Dong).

https://doi.org/10.1016/j.compositesb.2023.110632
Received 20 August 2022; Received in revised form 6 December 2022; Accepted 19 February 2023
Available online 24 February 2023

[9]. The developed multifunctional lightweight composites are expected to significantly improve their operation ranges.

As a common architecture used for composite laminates [10] and conventional batteries, most of the multifunctional carbon fiber reinforced composites are based on a laminated battery structure and fabricated through conventional lay-up processes [10–12]. The fabrication was either achieved through embedding the thin-film lithium ion batteries into carbon fiber composites [13] or using high strength carbon fibers as battery components, e.g., current collectors [14] and negative electrode [15]. Two carbon fiber electrode layers are typically separated by an electrically insulating layer. Practical examples of these fabricated composite parts include the form of body panels for electric vehicles and structural components [9]. However, the multifunctional applications also present new challenges for fabrication of structural battery composites, which extend beyond the scope of conventional manufacturing approaches and often require customizable, unconventional form factors depending specific applications. The traditional lay-up process yields high manufacturing costs and long fabrication cycles, hindering the further implementation of structural battery composites.

Additive manufacturing (AM) of continuous carbon fiber reinforced composites has been extensively studied for its advantages in fabrication of complex structural components with customizability and high mechanical performance [16]. Coextrusion deposition is commonly used to 3D print continuous carbon fiber reinforced composites via in-nozzle impregnation [17]. The coextrusion-based approach enables a radically new 3D structural battery architecture [18,19]. After coating each single carbon fiber with solid polymer electrolyte (SPE), the SPE-coated carbon fibers are then embedded in cathode matrix materials and form a concentric battery structure, with each continuous carbon fiber acting as a micro-battery cell. It has been shown that the thin SPE coatings greatly reduced Li-ion transport distance and exhibited high reversible energy storage capacity [20]. Moreover, with carbon fiber of a few micrometers, the 3D structural battery design greatly increases contact area between electrolyte and active materials due to high specific surface area of carbon fiber micro-battery cells. Thus, it is expected to exhibit ultrahigh battery performance with high energy density per footprint area and high areal capacity [21]. Compared to the laminated structural battery composites, achieving energy storage at fiber level would also allow higher charging rates. The single carbon fiber was shown to charge faster [22] than fibers in a fiber tow/yarn [23]. A higher reversible capacity was also found for a single carbon fiber compared to a carbon fiber yarn, attributed to the bundle structure that increased difficulty to access and intercalate fibers internally in the fiber tows/yarns [24].

Despite the significant potentials of 3D carbon fiber structural battery design discussed above, this novel multifunctional design also poses great challenges in current manufacturing techniques. The previous AM techniques were mainly optimized toward mechanical performance for their structural applications. AM of multifunctional composites often needs to directly dope mechanically strong polymers with active and conductive fillers [25]. The polymers were therefore used as binder materials for structural battery composite parts. It has been shown [26] that to facilitate 3D printing of structural battery composites with carbon fibers, a large volume of polymer as binder was required to maintain printability, which hindered the electrical contact between conductive and active materials and thus was a key factor lowering the obtained electrochemical performance compared to conventional battery cells. On the other hand, while a higher amount of active and conductive materials may be used, they deteriorated the printability, causing clogging during coextrusion or hindering curing of the printed samples [25]. Large volumes of active and conductive materials, though enabling electrochemical functions, also compromised the structural aspect of the multifunctional composites, yielding a trade-off between electrochemical and mechanical performance [27]. It will be necessary to investigate how to simultaneously improve mechanical-electrochemical performance by 3D printing conditions. There is a knowledge gap in understanding the coextrusion deposition process for the structural battery composites.

In this study, we first introduce a slurry-based coextrusion method to 3D print structural battery composites. A solvent-based cathode slurry is prepared at varying binder contents and solid loadings. The cathode slurry is then coextruded with SPE-coated carbon fibers before being deposited in 3D space to obtain the final parts. Examples of various samples are presented and used in different multifunctional applications for demonstration. The rheological behavior of the cathode slurry is experimentally investigated at different binder contents and solid loadings to identify proper printability window. The corresponding electrochemical and mechanical performance are also characterized. A thorough microstructure characterization of the 3D printed composite samples is performed to evaluate the effects of binder contents and solid loadings on residual voids. To help understand the coextrusion process, a meso-scale computational fluid dynamics (CFD) simulation is also implemented to investigate fiber impregnation and void formation processes. The findings help understand how to improve both mechanical and electrochemical performance by the 3D printing conditions for electrically powered structural systems where high multifunctional performance are in strong demands.

2. Materials and methods

2.1. Material preparation

2.1.1. Carbon fibers

To be used in the structural battery composites, carbon fibers would perform various functions simultaneously, i.e., carrying mechanical loads and acting as both negative electrodes and current collectors. Polyacrylonitrile (PAN)-based fibers, commonly used in the structural batteries, were selected in this study due to their favorable electrochemical and mechanical properties [28]. As-received Toray T800HB (12000 filaments per rowing, continuous carbon fibers with a diameter of about 7 μm) was used in this study due to its excellent electrochemical capacity and high modulus. Carbon fiber tows were first dried in the vacuum oven at 120 °C for at least 4 h to remove moisture. It helps minimize the negative effect of moisture on the conductivity and lithium-ion intercalation capabilities and promotes polymer adhesion [29]. Moreover, drying will help improve printability by reducing fiber clumping during the proposed coextrusion-based AM process, which can be detrimental to the deposition quality and subsequently composite properties [30].

2.1.2. Solid polymer electrolyte coating

In this study, each carbon fiber was coated with a solid polymer electrolyte, which also worked as separator in the structural battery composites. This was achieved through a three-electrode electrocoating assembly following the previously developed procedure [18,19,25] (with more details provided in the Supplementary data). Methoxy polyethylene glycol (350) monomethacrylate (SR550) monomer with 1 M lithium perchlorate ($LiClO_4$ by Sigma-Aldrich) was used in this study. The monomer was chosen specifically for its high ionic conductivity of 1.5×10^{-7} S cm^{-1} (measured at 258 °C) with low stiffness (<1 MPa) of the produced polymer [20]. The favorable properties facilitate coextrusion of SPE-coated carbon fibers during the proposed AM process. $LiClO_4$ was selected due to its less sensitivity to atmospheric moisture and applications in lithium-ion batteries [31]. Dimethylformamide (DMF by Sigma-Aldrich) were used as solvent for the methacrylate systems [32]. In this study, a constant monomer-to-solvent ratio of 1:2 (by volume) was used in the electrocoating process. A SPE coating of about 2 μm thickness in Fig. S1 was obtained with a polarization time of 400 s.

2.1.3. Cathode slurry

A solvent-based cathode slurry was used for the proposed 3D printing method in this study. DMF was used as solvents for cathode constituent

materials, i.e., binder, electrically conductive and electrochemically active materials. Polyvinylidene fluoride (PVDF by Sigma Aldrich), commonly used in lithium-ion batteries, were selected as binder for cathode matrix materials. Lithium iron phosphate ($LiFePO_4$ by Sigma-Aldrich) was added as active material. $LiFePO_4$ was preferred over other transition metal oxides owing to its relatively high theoretical capacity, cycling stability, higher safety, low cost, and non-toxicity [33]. However, $LiFePO_4$ has poor electrical conductivity ($\sim 10^{-9}$ S/cm) and lithium diffusivity ($\sim 8 \times 10^{-18}$ m^2/s), which can be compensated if using with sufficiently large amount of carbon conductive additives to achieve desired electrical performance [34]. Previous studies [25] also suggested that a high electrical conductivity in the 3D printed polymer-based lithium-ion batteries was critical for achieving good capacity. Super P conductive carbon black (by Alfa Aesar), supplemented by MF80 milled short carbon fiber strands (by Carbiso), was used in this study as conductive materials for its low resistivity and its common applications for electrodes of lithium-ion batteries [35].

The cathode slurry was prepared by mixing finely ground (<5 μm particle size) $LiFePO_4$ with Super-P carbon, milled short carbon fibers, and PVDF along with the DMF solvent using the AR100 planetary centrifugal mixer (by ThinkyUSA) at 2000 RMP for 20 min at ambient temperature and pressure. The slurry was then defoamed and transferred to the syringes, which were further processed on a centrifuge to remove bubbles prior to 3D printing experiments.

2.2. 3D printing method

The schematics of the proposed AM method is showed in Fig. 1(a) with corresponding experimental setup shown in Fig. 1(b). This was achieved through a coextrusion deposition setup with processing parameters summarized in Table 1, where a coextrusion nozzle was used. The outer nozzle (1.2 mm in diameter) was connected to a horizontal dispenser, feeding the prepared cathode slurry. To improve fiber wetting conditions and thus fiber-matrix bonding within 3D printed composites, a vertical dispenser was also included, holding the identical cathode slurry, to achieve pre-impregnation of carbon fiber.

Table 1
Processing conditions used for 3D printing of structural battery composites.

Outer nozzle diameter	1.2 mm
Inner nozzle diameter	0.6 mm
Print speed	0.5 mm/s – 2 mm/s
Dispensing pressure	20 psi – 70 psi
Post-curing	80 °C for 24 h in a vacuum oven

During 3D printing process, the SPE-coated continuous carbon fibers were fed through the cathode slurry (bath) within the vertical dispenser before being fed through the inner nozzle (0.6 mm in diameter). The pre-impregnated (prepreg) SPE-coated carbon fibers were then coextruded with the cathode slurry fed through the outer nozzle under drag force. The coextrusion nozzle was also found to simultaneously increase the drag force due to improved fiber wetting that facilitated coextrusion process. Otherwise, drawing forces during deposition would damage the delicate SPE coating. Under pressurized air, the prepreg SPE-coated continuous carbon fibers was impregnated by the cathode slurry during the coextrusion process before being deposited on the substrate layer-by-layer to 3D print different geometries. The deposited samples were post-cured at 80 °C for 24 h in a vacuum oven to remove the DMF solvent. A maximum fiber volume fraction of 53% was obtained using the proposed printing method. It is worth noting that the proposed AM method here was different from previous studies [18,19], where no solvents were used, and the binder materials were either thermally cured or by photopolymerization. In contrast, curing was achieved by evaporating solvents within the deposited cathode slurry in this study.

Several different shapes of structural battery composite samples were prepared as shown in Fig. 1(c)–(e), all successfully lighting up LEDs. A printed disc-shaped sample was also used to power a digital caliper in

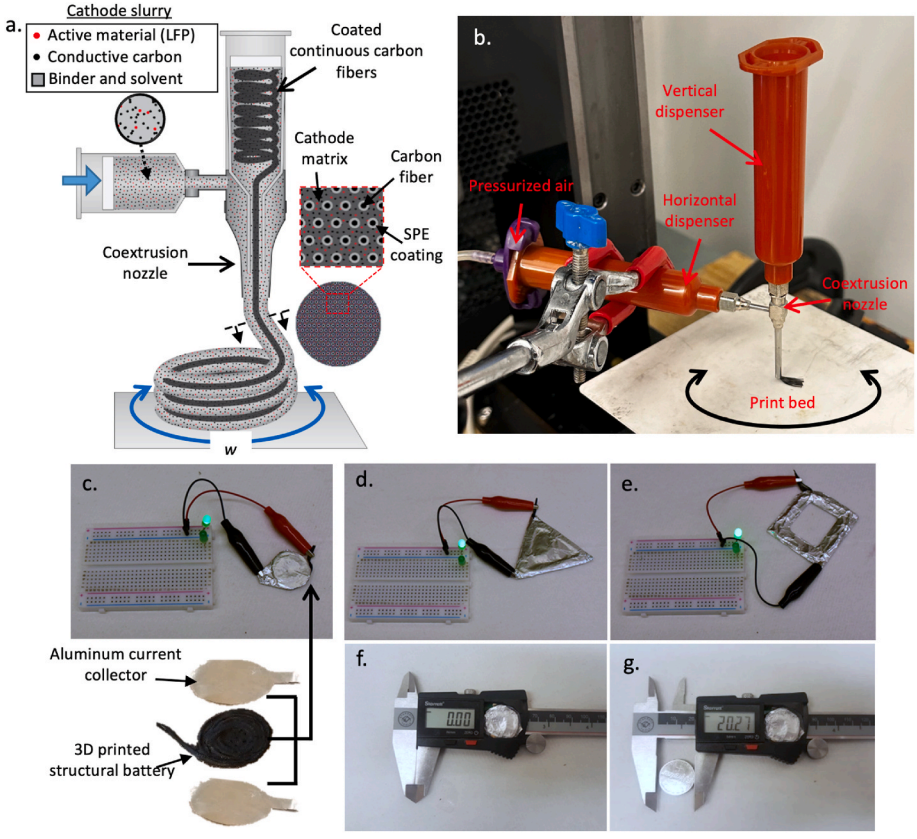

Fig. 1. Demonstrations of the proposed coextrusion deposition method and 3D printed structural battery composites samples. (a) shows the coextrusion deposition process of continuous carbon fibers with the cathode slurry, including electrically conductive materials (carbon black and milled carbon fibers), electrochemically active material (LFP), and binders (PVDF). (b) shows the experimental setup used for coextrusion deposition of structural battery composites. (c) shows a typical 3D printed disc-shaped structural battery composite sample, assembled with aluminum current collector, successfully powering an LED. (d)–(e) show additional 3D printed functional triangular- and square-shaped structural battery composite samples, demonstrating the capability of the proposed 3D printing method customizing battery form factor. (f)–(g) show the disc-shaped structural battery composite being used as a replacement for CR2032 lithium coin cell battery and powering a digital caliper.

Fig. 1(f) and 1(g) and Video S1 as well as a fan in Video S2. Additionally, a printed long-bar sample was also shown in Video S3 capable of simultaneously supporting mechanical bending loadings while powering an LED. These 3D printed samples well demonstrated the capabilities and flexibilities of the proposed 3D printing method in fabrication of functional structural battery composites as flexible power sources and customization of their battery form factor to fit specific needs of multifunctional applications [18,19].

Supplementary data related to this article can be found at https://doi.org/10.1016/j.compositesb.2023.110632.

2.3. Simulation setup

To investigate the effect of the cathode slurry on fiber impregnation and void formation, we also built a meso-scale 2D transient computational fluid dynamics model in COMSOL Multiphysics to analyze time-dependent coextrusion of SPE-coated carbon fibers and cathode slurry. A diameter of 7 μm was used for each carbon fiber. To improve computational efficiency, the carbon fiber tow was modeled by a representative volume element (RVE) of 100 μm × 100 μm based on our preliminary convergence tests. The fiber distribution was randomly generated with an effective porosity of 45% for the fiber tow in this study. To explicitly study the effect of cathode slurry on fiber impregnation process, it was modeled as a non-Newtonian power law fluid using the experimentally measured viscosity data below. The experimentally measured dynamic contact angles in Fig. S4 was also implemented for SPE-coated carbon fibers with varying cathode slurry compositions. A constant surface tension coefficient of 0.0371 N/m was used as the prepared cathode slurry was dominated by the DMF solvent. We modeled the Multiphysics analysis with a two-phase transient fluid flow using phase field method. The fluid-air interface was tracked to calculate the transient volume of the cathode slurry in the meso-scale domain to study time-dependent void formation and degree of impregnation.

2.4. Characterization

The viscosity of the prepared cathode slurry was measured by a viscometer (Brookfield model HB) equipped with a solid shaft SC4-27SD spindle at 25 °C. The galvanostatic charge-discharge curves and the electrochemical impedance spectra (EIS) of the 3D printed composite samples were obtained using a Gamry Reference 600+ potentiostat with a quick assembly split coin cell EQ-HSTC by MTI Corporation. For battery cycling, circular disc shaped samples (10 mm in diameter) were printed for testing. The capacities of the 3D printed samples were normalized by the cathode active materials. The tests were conducted within cut-off range between 4.5 V and 1 V. For EIS measurements, a frequency range of 10–10^6 Hz was used with an amplitude of 10 mV. 10 mm by 10 mm square samples were prepared and tested. The ionic conductivity was calculated as $\sigma = l/(AR_b)$, where l is the thickness, A is the cross-sectional area of the printed square samples, and R_b is the bulk resistance acquired through the intercept with real axis from Nyquist plot [36]. The electrical resistivity was measured using a Signatone Pro4-4000 Four Point Resistivity System with Keithley 2400 Sourcemeter. To evaluate mechanical performance, tensile setup in Fig. S2 following ASTM D3039 were used to test five printed samples of each type with specimen geometry of 100 mm × 3 mm × 1 mm on an Instron 5881 tester. A constant strain rate of 0.01/min was applied until sample failure. The measured tensile force and displacement were then used to calculate the engineering stress and strain results in this study. It is worth noting that as the developed new structural battery composite integrated the functions of both electrical energy storage and load bearings in a single material, both electrochemical and mechanical properties were evaluated in this study for energy storage and structural applications. Microstructure characterization was performed on the cross-section of each sample printed with varying cathode slurry composition. The printed samples were sectioned using a slow-speed diamond saw and polished using diamond polishing discs of up to 3 μm in grit size. The cross-sectional images were then taken by scanning electron microscopy (SEM) using a Quanta 600F Environmental Scanning Electron Microscope to characterize the composite microstructure. At least three different locations were observed to collect typical 3D printed microstructure.

3. Results and discussion

Achieving a uniform dispersion of SPE-coated carbon fibers and active materials (LFP) within cathode matrix is critical for the proposed 3D structural battery composites. Thus, we first characterized the composite microstructure to confirm successful 3D printing of the proposed structural battery architecture in Fig. 2(a). Each individually SPE-coated carbon fiber within the fiber tow was expected to embed within cathode matrix, where carbon fiber worked as negative electrode and SPE coating worked as solid electrolyte and separator, forming a network of carbon fiber micro-batteries. A typical SEM microscopic image of the obtained composite microstructure is shown in Fig. 2(b). SPE-coated carbon fibers were dispersed within the porous cathode matrix, where PVDF and LFP were used as binder and active materials, respectively. It should be noted that the nonuniform dispersion of carbon fibers could be improved through either spreading SPE-coated carbon fibers before 3D printing or more accurately controlling fiber extrusion during 3D printing, e.g., with vibration-assist on coextrusion head or print bed. A close-up view of a single carbon fiber is highlighted in Fig. 2(c) with SPE coating. It is worth noting that the SPE coating shown here was damaged during post-processing 3D printed samples for microstructural characterization. Previous studies [18,19] showed that the coextrusion deposition method would obtain intact SPE coating within the 3D printed samples, serving as both electrolyte and separator to avoid short-circuiting. The results were further confirmed in this study by the collected discharge results in Fig. 2(d), which would otherwise show short-circuiting. The voltage profiles indicate a stable discharge process. The 3D printed samples were found to show stable electrochemical charge/discharge processes up to 100 cycles in Fig. 2(e). All the tested samples experienced a large irreversible capacity loss within the first 5 cycles, attributed to the formation of solid electrolyte interphase layer and trapped Li within the carbon fibers [37]. After stabilization, an average discharging capacity of 35 mAh/g was obtained with good capacity retention observed over long-term cycling. An average Coulombic efficiency of 80% was still maintained after 100 charge/discharge cycles. We also found that the printed samples showed relatively stable electrochemical capacities within the given cycling process at different C-rates in Fig. 2(f), further confirming the successful preparation of functional structural battery composites. The energy density of the stabilized battery at C/2 was 77 Wh/kg with a nominal voltage of 2.2 V during discharge. The obtained energy density was over three-fold of those reported in previous studies [19,25] of 3D printed structural battery composites. The significant improvement was attributed to a much higher level of conductive and active materials within cathode as enabled by the slurry-based coextrusion deposition method in this study. Previous studies [25,26] suggested that a high amount of binder materials was typically needed to achieve 3D printing of battery samples. Due to the presence of high percentage of binder materials, a low ratio of active to conductive materials was also needed to improve the electrical contact between conductive and active materials. In contrast, with a minimum binder content of 25% (over a minimum of 40% in previous studies [19,25]), a higher ratio of active to conductive materials at 1.5 (over a ratio of 0.25 in previous studies [19,25]) was achieved without compromising printability for the proposed 3D printing method in this study, further promoting the obtained electrochemical performance.

Previous studies [5] suggested a cathode constituent composition of $LiFePO_4$:Super-P carbon:PVDF at a weight ratio of 54:34:12. However,

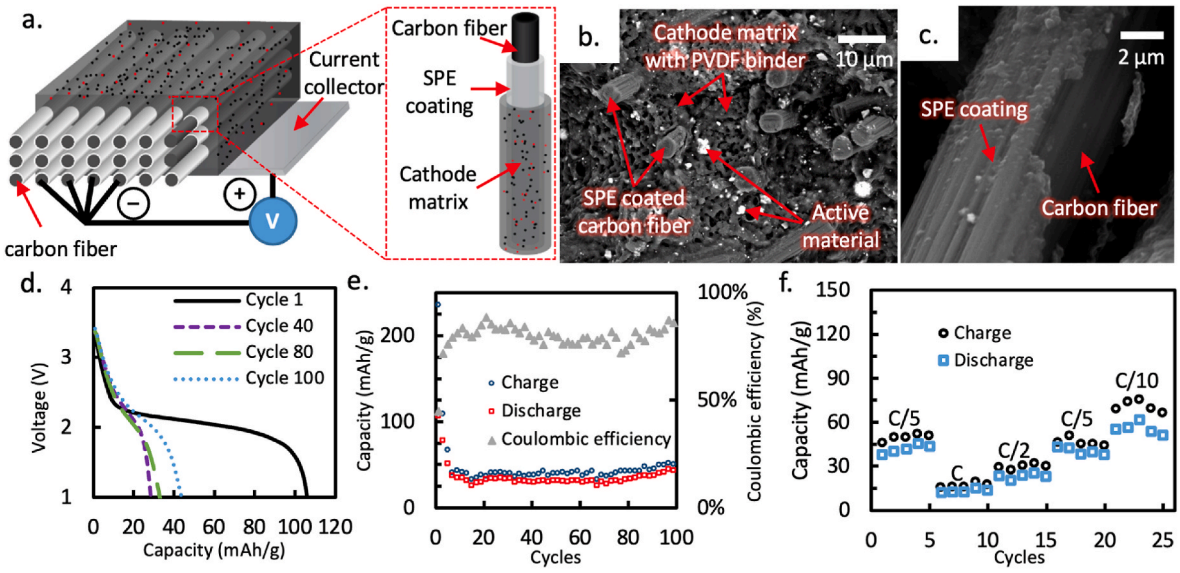

Fig. 2. Characterization of the structural battery composites prepared by the proposed 3D Printing method. (a) shows the expected 3D structural battery composite architecture. Each carbon fiber is coated with SPE and distributed within cathode matrix materials, working as a micro-battery as shown in the close-up view. (b) shows the SEM image of the obtained structural battery composite samples. SPE-coated carbon fibers are distributed within porous cathode matrix using PVDF as binder. Active material (LFP) is also observed as bright particles distributed across the porous matrix. (c) highlights a typical individual carbon fiber with SPE coating. (d) shows the typical discharge curves up to 100 cycles for the 3D printed samples. (e) shows the charge and discharge capacities and Coulombic efficiency at C/5 for 100 cycles. A disc-shaped sample printed with a solid loading of 1:5 and a binder content of 25% was tested. (f) shows the cycling results at varying C-rates.

the corresponding poor structural integrity, with poor printability, made it extremely difficult to additively manufacture structural parts in our preliminary tests. To this end, one alternative approach is to directly increase the binder content for improved bonding strength [38], which however would lower the electrochemical performance of the prepared electrode materials by hindering the electrical contact between conductive and active materials. Thus, to minimize the necessity of using excessive binder content, conductive milled short carbon fibers were introduced in this study as supplementary conductive material due to improved structural integrity found in our preliminary tests to facilitate the proposed AM process. Moreover, the increased aspect ratio of the selected conductive fillers (i.e., milled short carbon fibers) was also found to improve the cathode electrical conductivity due to reduced sensitivity to inter-particle contact within the formed particulate/fibrous network [33], further promoting electrochemical performance. Preliminary parametric studies were then performed by varying ratio of active material to conductive material to achieve maximum energy capacity. A slurry consisting of $LiFePO_4$, Super-P carbon, Milled short carbon fiber, and PVDF at a ratio of 45:12:18:25 by weight was found to exhibit highest capacities while still maintaining good structural integrity with a minimum amount of binder content (PVDF) used. The effect of binder contents was also further studied by varying PVDF from 25% to 45% to study the corresponding electrochemical performance, mechanical properties, and microstructure of the additively manufactured structural battery composite samples.

It is also worth noting that while the introduction of milled short carbon fibers improved the structural integrity, it would also lower the printability due to increased clogging tendency for the proposed coextrusion approach. It is typically related to the slurry viscosity, as controlled by the solid loading, i.e., the cathode constituent materials in DMF (as solvent) in this study. A maximum solid loading represented by cathode-to-DMF ratio at 1:3 (by volume) was found to avoid clogging. A minimum ratio of 1:5 was necessary to avoid noticeable sagging and to maintain print resolution for the 3D printed samples.

Using the proposed coextrusion-based printing method, the cathode slurry is thus a key factor in the development of printable carbon fiber structural battery composites. A high concentration of cathode constituent materials may cause clogging of the printing nozzle and sagging during deposition, both of which would lower the quality of the final parts. To this end, the rheological profile of the cathode slurry is critical in determining its ability to flow through the printing nozzle, impregnate the carbon fiber bundle, and maintain structural integrity after deposition, i.e., its printability into solid composite samples. Thus, we first analyzed and summarized the typically measured rheological behavior of the cathode slurry with varying binder contents and solid loadings in Fig. 3. All prepared cathode slurries clearly exhibited a typical shear-thinning behavior as characterized by decreasing viscosity with increasing shear rates, regardless of binder contents in Fig. 3(a) and solid loadings in Fig. 3(c). The behavior was desirable for the proposed 3D printing method as the applied high pressure would facilitate coextrusion and fiber impregnation during coextrusion and the deposited samples could easily maintain structural integrity for post-curing.

On the other hand, as shown in Fig. 3(a) and (c), an increase in viscosity was found while increasing binder contents or solid loadings. The required pressure air may exceed the maximum pressure that can be achieved using the existing 3D printer setup, making the cathode slurry not printable. Thus, the printing process-related shear-stress and shear-rate limits were also calculated, i.e., to determine the proper printability window in Fig. 3 (b) and 3(d) using a capability flow model (with more details in reference [39]). The measured rheological behavior was also included for the cathode slurry with varying compositions for comparison. The process-related shear-stress was estimated based on the applied pressure and the nozzle geometry [40]. Using the proposed printing method, we found that applying a pressure higher than 70 psi would lead to cathode material sagging after deposition while a pressure lower than 20 psi would be inadequate to coextrude carbon fiber tow with the cathode slurry. Thus, the allowable-process related shear-stress range was found to be between 1.5 kPa and 10 kPa in Fig. 3(b) and (d). Similarly, the process-related shear rate was estimated from the flow rate of the cathode slurry (related to print speed) after considering the Rabinowitch-Mooney correction factor for non-Newtonian fluid [39]. Using the existing coextrusion nozzle, we found that a print speed higher than 0.5 mm/s yielded a discontinuous deposition while a print speed higher than 2 mm/s led to poor printing resolution. An allowable process-rated shear rate was thus obtained within the range of 0.5 s^{-1} and 10.2 s^{-1}. It should be noted that the obtained printability windows

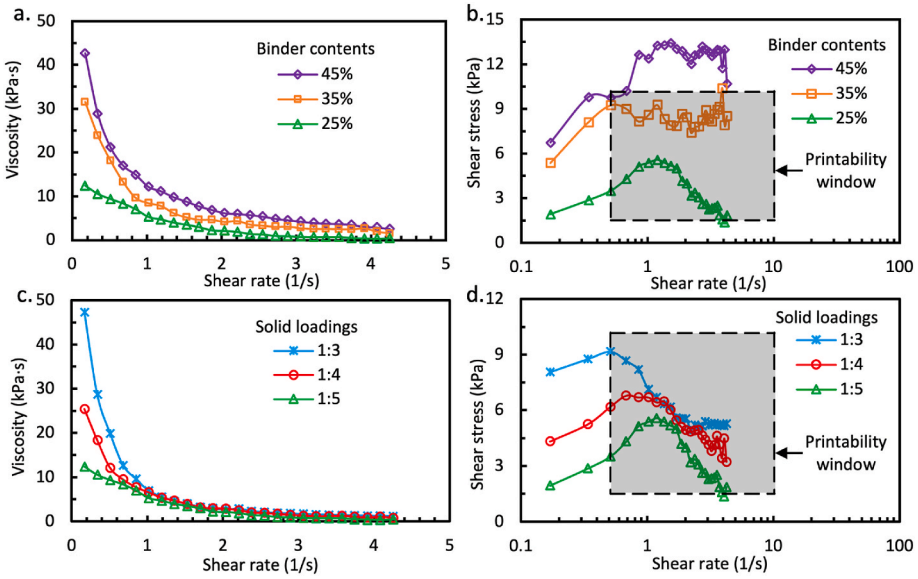

Fig. 3. Rheology characterization of the cathode slurry with varying compositions. (a) and (c) show the measured viscosity curves at different binder contents and solid loadings, respectively. (b) and (d) show the measured shear stress in terms of shear rate for varying binder contents and solid loadings, respectively. The estimated printability windows are also included as the areas within the dashed lines.

in Fig. 3(b) and (d) could be expanded by improving the coextrusion nozzle or printing environments.

As seen in Fig. 3(b), after addition of binder contents to 45%, the rheological curve quickly moved outside the printability window, showing a finite overlap with the printability window, specifically, close to a shear stress of 10 kPa and a shear rate of 0.5 s^{-1}. Correspondingly, only a high pressure at 70 psi with a low print speed of 0.5 mm/s could be used to 3D print structural battery composite samples with 45% binders using the existing setup. In order to compare all different cathode slurry compositions attainable within the printability window, a pressure of 70 psi and a print speed of 0.5 mm/s were thus used for further characterization below. This was also how a maximum of 45% was selected for the binder contents in this study. In comparison, we found that varying solid loading was a more effective way of controlling printability of the cathode slurry, showing a wide range of proper process-related shear stress (related to applied pressure) and shear rate (related to print speed). These findings were further confirmed by printing structural battery composite samples using varying cathode slurries.

The obtained electrochemical performance of different printed structural battery composite samples was first compared. As the electrochemical capacity was found to stabilize within 10 cycles, we tested all the samples for 10 cycles at C/5 and used the typical 10th cycle results for comparative studies of different cathode slurry compositions in Fig. 4(a) and Fig. 4(c) with varying binder contents and solid loadings, respectively. With the addition of binder contents, the specific capacity consistently decreased from 35 mAh/g to 14 mAh/g in Fig. 4(b). This was expected as increasing binder contents reduced ionic conductivity and increased electrical resistivity of the cathode matrix as shown in Fig. S3. In contrast, just changing solid loadings while using a same

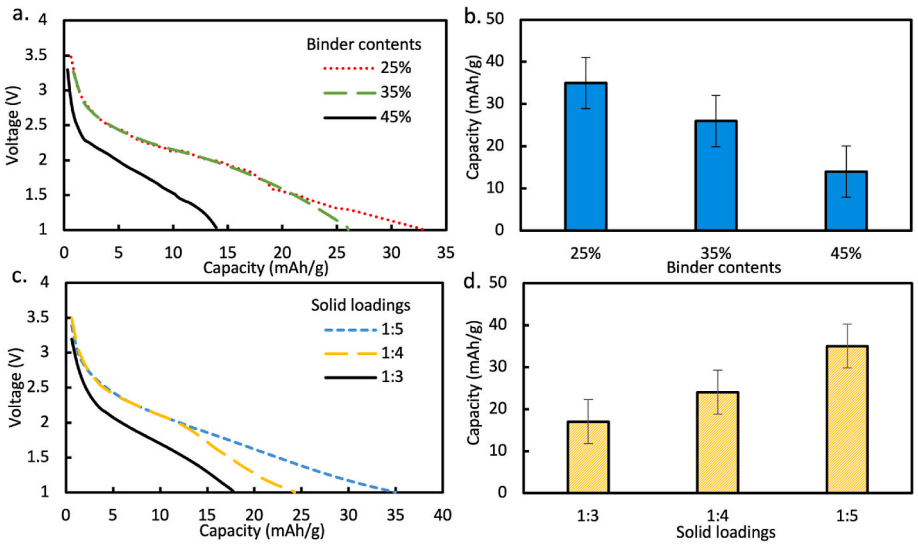

Fig. 4. Electrochemical characterization of 3D printed structural battery composites with varying cathode slurry compositions. (a) and (c) show typical the 10th cycle discharge curves for varying binder contents and solid loadings, respectively. Only three different combinations are shown for clarification. (b) compares the obtained specific capacities with binder contents ranging between 25% and 45%. (d) compares the obtained capacities with solid loadings varying between 1:3 and 1:5.

binder content was not expected to vary cathode ionic conductivity and electrical resistance due to a fixed cathode constituent composition in 3D printed samples. We found that changing solid loadings just varied the electrical resistivity between 0.2 Ω cm and 0.4 Ω cm while a consistent ionic conductivity of 11 mS cm^{-1} was measured for the printed cathode. However, as clearly seen in Fig. 4(d), decreasing solid loading significantly improved the obtained specific capacity. An improvement of 106% was achieved after decreasing solid loading from 1:3 to 1:5. We believe the improvement was mainly attributed to the lowered viscosity for the cathode slurry at lower solid loadings as observed in Fig. 3(c). A lower viscosity was expected to facilitate fiber impregnation and lower residual void fraction, which in turn would decrease the resistance between SPE-coated carbon fibers and cathode matrix. On the other hand, the increased viscosity at higher binder contents may also contribute to the lower capacities in Fig. 4(b) due to higher residual void fraction. These were further confirmed by detailed microstructure characterization below for the samples printed with varying cathode slurry compositions.

The mechanical performance of the printed structural battery composites was also a key factor as they were expected to support mechanical loadings while working as an electrical energy source. The typical stress-strain curves from tensile testing were shown in Fig. 5(a) for composite samples printed with varying binder contents. As expected, increasing binder contents within cathode matrix increased maximum tensile stress. The measured tensile strength and tensile modulus were improved by 41% and 51%, respectively, after increasing binder contents from 25% to 45%. It should be noted that increasing binder contents, in the meantime, lowered the obtained capacities as seen above in Fig. 4(b). These indicated that merely varying binder contents followed a typical trade-off trend observed for structural battery composites [41], where improving mechanical performance would yield lower electrochemical performance, and vice versa.

On the other hand, we found that lowering solid loadings increased mechanical performance in Fig. 5(c) while simultaneously improving electrochemical capacities seen in Fig. 4(d). The measured tensile strength and modulus were increased by 108% and 40% after reducing solid loadings from 1:3 to 1:5 for the cathode slurry used for 3D printing of structural battery composites. This indicated that lowering solid loadings during 3D printing helped improve both mechanical and electrochemical performance, providing an effective fabrication approach of "breaking" the trade-off typically observed for structural battery composites. We believe that the improvement was mainly attributed to the residual voids within the fabricated composite samples as further analyzed in detail below from microstructure characterization.

It is also worth noting that carbon fibers here were not only used as battery components but also as reinforcement for the structural battery composites. The tensile strength and modulus of the cathode matrix printed with 25% binders were found to be just 7 MPa and 27 MPa, respectively. In contrast, the introduction of carbon fiber reinforcements greatly improved the mechanical performance with a maximum of 1.1 GPa and 124 GPa obtained for tensile strength and tensile modulus, respectively.

To evaluate the effect of residual voids on 3D printed composite samples, the microstructure for varying binder contents was first characterized with typical microscopic images shown in Fig. 6(a)-(c). A growing number of voids was observed after increasing the binder contents from 25% to 45%. These voids were further highlighted similar to Fig. 6(c) and used to obtain the total void fraction in Fig. 6(d). Three different locations within the composites were examined under SEM for estimation of the void fraction. Increasing binder contents notably increased the void fraction from 2.9% to 4.8%. The increased residual void fraction is attributed to be increased shear stress at increased binder contents as shown in Fig. 3(b), which makes it more difficult for the cathode slurry to impregnate the carbon fiber network as also studied below through numerical simulations. The increasingly trapped voids are expected to further increase the resistance between SPE-coated carbon fibers and cathode matrix materials, contributing to the lower capacities measured in Fig. 4(b). While increasing binder contents was still clearly seen to improve obtained mechanical performance in Fig. 5(b), its contribution may have been offset by the increasing residual voids as defects left within the printed composite samples. We expect that reducing void formation will help further improve the obtained tensile strength and modulus above. Further detailed examination of void size distribution in Fig. 6(e) showed that the residual voids was dominated by small voids. We believe this is closely related to fiber impregnation during coextrusion deposition of cathode slurry with SPE-coated carbon fibers. While most voids were expected to combine into large voids and removed during fiber impregnation, smaller voids tended to be trapped within the printed composite samples, attributed to a limited amount of impregnation time at the given print speed (0.5 mm/s) during coextrusion before the extrudate was deposited. While further

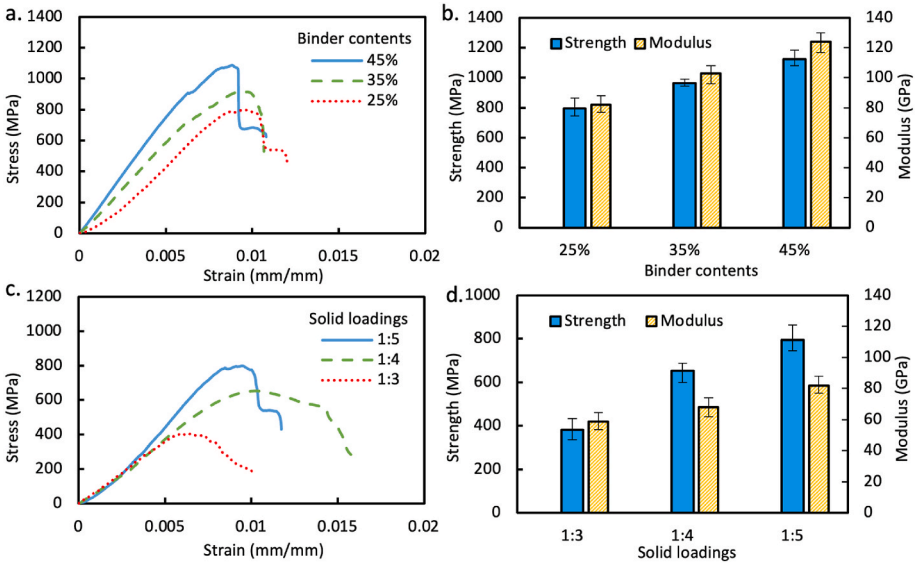

Fig. 5. Mechanical characterization of 3D printed structural battery composites. (a) and (c) show typical stress-strain curves measured from tensile testing of 3D printed samples with varying binder contents and solid loadings, respectively. Only three different combinations are shown for clarification. (b) and (d) compare the measured tensile strength and modulus for varying binder contents and solid loadings, respectively.

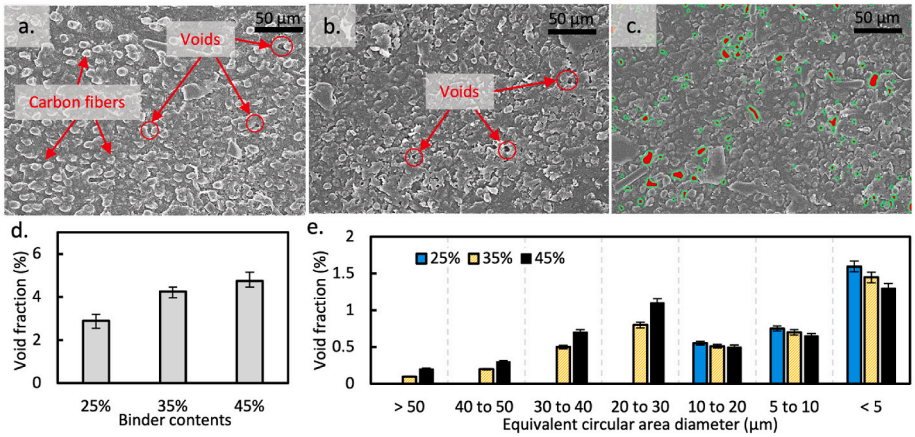

Fig. 6. Microstructure characterization of 3D printed structural battery composites in terms of binder contents. Typical microscopic images are shown for binder contents of 25%, 35%, and 45% in (a), (b), and (c), respectively. The typical highlighted voids similar to (c) are used to estimate total void fraction in (d) and void size distribution in (e) for the printed samples.

lowering print speed can increase the fiber impregnation time, it will also lower the fabrication efficiency and even make the samples unattainable due to poor printability. It is also observed in Fig. 6(e) that the increased void fraction at higher binder contents was mainly attributed to increased large residual voids. The higher viscosity at higher binder contents may lower impregnation rate with larger voids more easily trapped within the printed samples. Thus, it will be necessary to further investigate how to improve fiber impregnation while maintaining a same print speed.

Using the same print speed, reducing solid loadings from 1:3 to 1:5 was found to greatly reduce the residual voids in Fig. 7(a)-(c). A reduction of 49% in residual void fraction was observed as summarized in Fig. 7(d). While the residual void fraction was still dominated by small voids, most of large voids have been eliminated at the solid loading of 1:5 as seen in Fig. 7(e). The finding, combined with measured mechanical and electrochemical performance above, showed the advantage of using a lower solid loading within the cathode slurry. The proposed micro-battery architecture in Fig. 2(a) highly depends on the surface contact between SPE-coated carbon fibers and cathode matrix materials (including binders to support mechanical loading as well as active and conductive materials for electrical energy storage). A significant decrease in residual voids after decreasing the solid loading would increase the contact area between SPE-coated carbon fibers and cathode materials and lower the SPE-cathode interfacial resistance, thus promoting the obtained capacities during battery cycling. In the meantime, the improved bonding between SPE-coated carbon fibers and cathode matrix materials would also promote the fiber reinforcement and corresponding measured mechanical performance. It should be noted that although varied solid loadings within the cathode slurry were used for 3D printing, the cathode constituent materials remained the same, i.e., a ratio of $LiFePO_4$, Super-P carbon, Milled short carbon fiber, and PVDF at 45:12:18:25 by weight. This indicated that the improvements in both mechanical and electrochemical performance were governed by the reduction in residual void fraction within 3D printed sample. We believe that the greatly reduced void fraction is affected by the degree of impregnation during coextrusion deposition of SPE-coated carbon fibers and cathode slurry, which is closely related to the cathode slurry rheological behavior.

The effect of the cathode slurry on void formation was further studied through the meso-scale 2D transient computational fluid dynamics model as demonstrated in Fig. 8(a)-8(c) to investigate time-dependent fiber impregnation process during coextrusion of SPE-coated carbon fibers and cathode slurry. The time-dependent void formation and degree of impregnation was studied through tracking the fluid-air interface in Fig. 8(a)-8(c) and calculating the transient volume of the cathode slurry in the meso-scale domain. The fiber impregnation mechanism was found to be dominated by viscous effect, where the majority of the slurry motive force came from the fluid wetting the fiber walls and the resulting capillary action. It was further confirmed by the estimated Reynold's number, a ratio of inertial force to viscous force, to

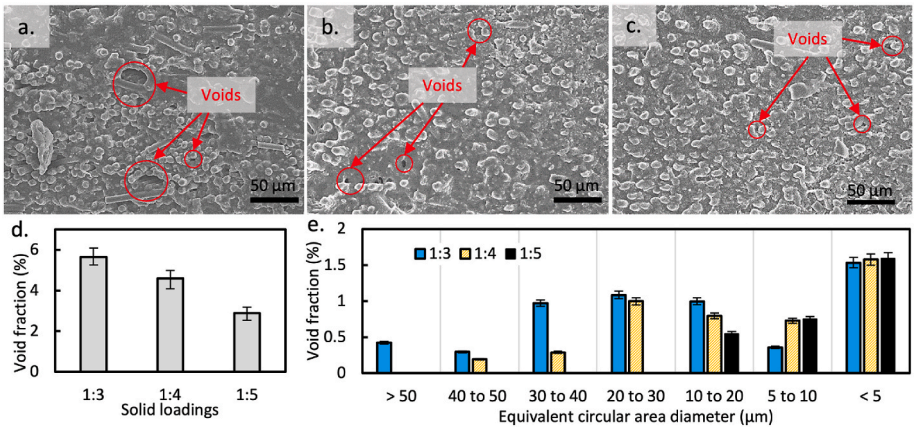

Fig. 7. Microstructure characterization of 3D printed structural battery composites in terms of solid loadings. Typical microscopic images are shown for solid loadings of 1:3, 1:4, and 1:5 in (a), (b), and (c), respectively. The estimated void fraction is summarized in (d). The weighted histogram in (e) shows the variation in void size distribution within structural battery composite samples printed with varying solid loadings.

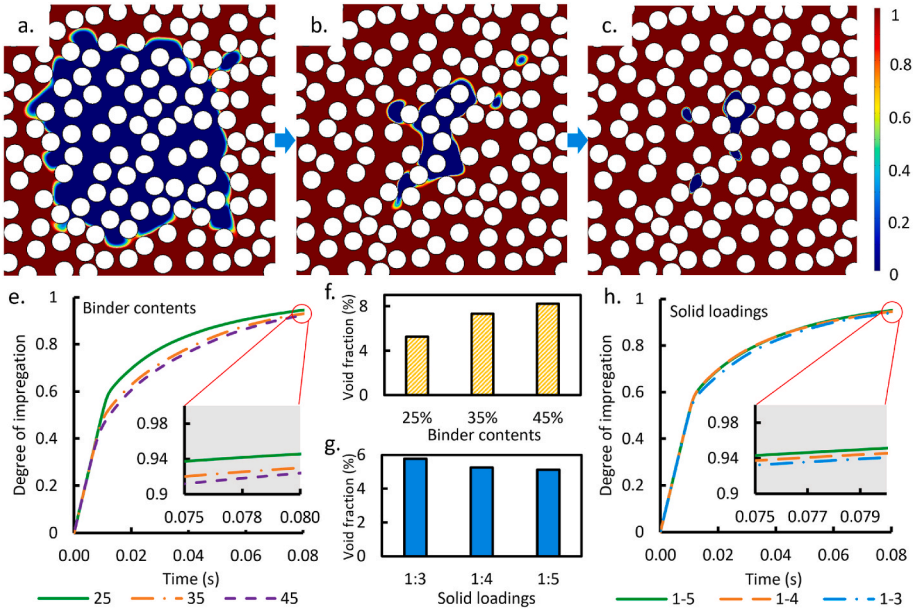

Fig. 8. Meso-scale computation fluid dynamics simulations of fiber impregnation during coextrusion of cathode slurry with SPE-coated carbon fibers. (a)–(b) show the simulated contours of cathode slurry volume fraction for time-dependent fiber impregnation and void formation processes. (c) shows a typical residual void distribution near the end of coextrusion. A binder content of 45% with a solid loading of 1:5 is used here for demonstration. (e) and (h) show the degree of impregnation over time for varying binder contents and solid loadings, respectively. The inlet images show close-up views of degree of impregnation near the end of 3D printing process. (f) and (g) summarize the total residual void fraction for different binder contents and solid loadings, respectively.

be just 1×10^{-6}. This was closely related to the relatively low porosity of fiber tow, promoting capillary effect.

Visible void formation was also clearly seen in Fig. 8(a)-8(b), attributed to the slurry quickly wetting surrounding fibers and trapping air bubbles. The degree of impregnation gradually increased over time in Fig. 8(e) and (h) as the impregnation rate became lower. Further fiber impregnation eliminated certain voids while others was left as residual voids in Fig. 8(c) within the 3D printed composite microstructure. We expect that a longer impregnation time would improve the degree of impregnation and eventually remove these residual voids. However, with the given print speed, fiber impregnation would only have limited amount of time before the extrudates of SPE-coated carbon fibers and cathode slurry were deposited. Based on our experimental setup in this study, the coextrusion process took only 0.08 s before being deposited on the print bed for the scaled RVE in Fig. 8, limiting the degree of impregnation that can be achieved. These predicted void characteristics in Fig. 8(c) also well captured the typically observed residual voids within 3D printed multifunctional composite microstructure in Figs. 6 and 7.

In the meantime, the degree of impregnation was also affected by the cathode slurry compositions. As seen in Fig. 8(e), increasing binder contents reduced the impregnation rate and the degree of impregnation under the same print speed. A much higher residual void fraction was also predicted in Fig. 8(f). On the other hand, lowering the solid loading was found to slightly increase the impregnation rate and the degree of impregnation in Fig. 8(h). The predicted residual void fraction was reduced from 5.8% to 5.1% after decreasing the solid loadings from 1:3 to 1:5 in Fig. 8(g). It is worth noting that as the same experimental conditions were used here, the predicted residual void fraction in Fig. 8 (f) and (g) can be directly compared with experimental measurements in Figs. 6(d) and 7(d), respectively. While similar trends were observed, the predicted values were generally higher than the experimental results. The discrepancy is attributed to the fact that the developed meso-scale simulation here only considered the coextrusion process, limiting the total amount of simulated fiber impregnation time. However, in actual 3D printing experiments, further fiber impregnation may still happen within the deposited samples as the solvent being evaporated and further removed during post-curing, thus lowering the residual void fraction. This may also explain why more significant reduction in residual void fraction (from 5.7% to 2.9%) was observed from our experimental measurements after decreasing solid loading in Fig. 7(d). A lower solid loading indicated the presence of more solvents within the deposited composite samples, which would typically take longer time to be removed and thus allow more fiber impregnation time.

4. Conclusion

In summary, this study presented experimental and numerical studies of a slurry-based coextrusion deposition method to additively manufacture carbon fiber structural battery composites. The cathode slurry was coextruded and deposited with SPE-coated carbon fibers before post-cured to obtain the composite samples. Examples of various complex 3D geometries were demonstrated to successfully power electronic devices and support mechanical loadings. Characterization of the rheological properties of the cathode slurry showed that the binder contents and solid loadings determined the printability of the proposed printing method. Increasing binder contents improved mechanical performance but lowered the obtained electrochemical capacities. Varying solid loadings was found to be an effective way of simultaneously improving electrochemical and mechanical properties of the 3D printed structural battery composites. The electrochemical capacity was improved by 106% after decreasing the solid loading from 1:3 to 1:5. In the meantime, the tensile strength and modulus were also greatly improved by 108% and 40%, respectively. The improvement was attributed to be lowered residual voids as characterized by microscopic images of the 3D printed samples, and improved fiber impregnation as further examined by the meso-scale CFD simulations. Increasing binder contents from 25% to 45% increased residual void fractions from 5.3% to 8.2%, combined with increased resistance, led to lower electrochemical capacities. The predicted residual void fraction was reduced from 5.8% to 5.1% after decreasing the solid loadings from 1:3 to 1:5. This study showed that varying solid loadings of the cathode slurry was an effective way of improving printability, mechanical and electrochemical properties of the carbon fiber structural battery composites without varying cathode constituent materials. The residual voids were also found to play a key factor in the multifunctional performance of the 3D printed structural battery composites. With each carbon fiber working as a micro-battery, further improvement in degree of impregnation would enhance the surface contact area between SPE-coated carbon fibers and cathode matrix materials, potentially improving both electrochemical and mechanical properties. Thus, it will be worth future studies on how to further enhance the performance of structural

battery composites and promote their multifunctional applications.

Author statement

Aditya R. Thakur: Data curation; Investigation; Methodology; Visualization; Roles/Writing - original draft. **Xiangyang Dong:** Conceptualization; Data curation; Funding acquisition; Investigation; Methodology; Project administration; Resources; Roles/Writing - original draft; Writing - review & editing.

Declaration of competing interest

The authors declare that they have no known competing financial interests or personal relationships that could have appeared to influence the work reported in this paper.

Data availability

Data will be made available on request.

Acknowledgments

The authors gratefully acknowledge the supports from the Intelligent Systems Center at Missouri University of Science and Technology and AFOSR grant FA9550-21-1-0226.

Appendix A. Supplementary data

Supplementary data to this article can be found online at https://doi.org/10.1016/j.compositesb.2023.110632.

References

[1] Xu J, Geng Z, Johansen M, Carlstedt D, Duan S, Thiringer T, Liu F, Asp LE. A multicell structural battery composite laminate. EcoMat 2022:e12180. **n/a**(n/a.
[2] Luo Y, Li Y, Sharma P, Shou W, Wu K, Foshey M, Li B, Palacios T, Torralba A, Matusik W. Learning human–environment interactions using conformal tactile textiles. Nat Electronic 2021;4(3):193–201.
[3] Jacques E, Lindbergh G, Zenkert D, Leijonmarck S, Kjell MH. Piezo-electrochemical energy harvesting with lithium-intercalating carbon fibers. ACS Appl Mater Interfaces 2015;7(25):13898–904.
[4] Johannisson W, Harnden R, Zenkert D, Lindbergh G. Shape-morphing carbon fiber composite using electrochemical actuation. Proc Natl Acad Sci USA 2020;117(14):7658.
[5] Asp LE, Johansson M, Lindbergh G, Xu J, Zenkert D. Structural battery composites: a review. Function Composite Struct 2019;1(4):042001.
[6] Carlstedt D, Asp LE. Performance analysis framework for structural battery composites in electric vehicles. Compos B Eng 2020;186:107822.
[7] Adam JT, Liao G, Petersen J, Geier S, Finke B, Wierach P, Kwade A, Wiedemann M. Multifunctional composites for future energy storage in aerospace structures. Energies 2018;11(2).
[8] Capovilla G, Cestino E, Reyneri LM, Romeo G. Modular multifunctional composite structure for CubeSat applications: preliminary design and structural analysis. Aerospace 2020;7(2):17.
[9] Johannisson W, Zenkert D, Lindbergh G. Model of a structural battery and its potential for system level mass savings. Multifunct Mater 2019;2(3):035002.
[10] Senokos E, Ou Y, Torres JJ, Sket F, González C, Marcilla R, Vilatela JJ. Energy storage in structural composites by introducing CNT fiber/polymer electrolyte interleaves. Sci Rep 2018;8(1):3407.
[11] Yu Y, Zhang B, Feng M, Qi G, Tian F, Feng Q, Yang J, Wang S. Multifunctional structural lithium ion batteries based on carbon fiber reinforced plastic composites. Compos Sci Technol 2017;147:62–70.
[12] Moyer K, Boucherbil NA, Zohair M, Eaves-Rathert J, Pint CL. Polymer reinforced carbon fiber interfaces for high energy density structural lithium-ion batteries. Sustain Energy Fuels 2020;4(6):2661–8.
[13] Pattarakunnan K, Galos J, Das R, Mouritz AP. Tensile properties of multifunctional composites embedded with lithium-ion polymer batteries. Compos Appl Sci Manuf 2020;136:105966.
[14] Moyer K, Meng C, Marshall B, Assal O, Eaves J, Perez D, Karkkainen R, Roberson L, Pint CL. Carbon fiber reinforced structural lithium-ion battery composite: multifunctional power integration for CubeSats. Energy Storage Mater 2020;24:676–81.
[15] Johannisson W, Ihrner N, Zenkert D, Johansson M, Carlstedt D, Asp LE, et al. Multifunctional performance of a carbon fiber UD lamina electrode for structural batteries. Compos Sci Technol 2018;168:81–7.
[16] Todoroki A, Oasada T, Mizutani Y, Suzuki Y, Ueda M, Matsuzaki R, Hirano Y. Tensile property evaluations of 3D printed continuous carbon fiber reinforced thermoplastic composites. Adv Compos Mater 2020;29(2):147–62.
[17] Matsuzaki R, Ueda M, Namiki M, Jeong T-K, Asahara H, Horiguchi K, Nakamura T, Todoroki A, Hirano Y. Three-dimensional printing of continuous-fiber composites by in-nozzle impregnation. Sci Rep 2016;6:23058.
[18] Thakur A, Dong X. Printing with 3D continuous carbon fiber multifunctional composites via UV-assisted coextrusion deposition. Manufacture Lett 2020;24:1–5.
[19] Thakur A, Dong X. Additive manufacturing of 3D structural battery composites with coextrusion deposition of continuous carbon fibers. Manufacture Lett 2020;26:42–7.
[20] Leijonmarck S, Carlson T, Lindbergh G, Asp LE, Maples H, Bismarck A. Solid polymer electrolyte-coated carbon fibres for structural and novel micro batteries. Compos Sci Technol 2013;89:149–57.
[21] Asp LE, Greenhalgh ES. Structural power composites. Compos Sci Technol 2014;101:41–61.
[22] Kjell MH, Zavalis TG, Behm M, Lindbergh G. Electrochemical characterization of lithium intercalation processes of PAN-based carbon fibers in a microelectrode system. J Electrochem Soc 2013;160(9):A1473–81.
[23] Kjell MH, Jacques E, Zenkert D, Behm M, Lindbergh G. PAN-based carbon fiber negative electrodes for structural lithium-ion batteries. J Electrochem Soc 2011;158(12):A1455–60.
[24] Asp LE, Leijonmarck S, Carlson T, Lindbergh G. Realisation of structural battery composite materials. 2015.
[25] Pappas JM, Thakur AR, Dong X. Effects of cathode doping on 3D printed continuous carbon fiber structural battery composites by UV-assisted coextrusion deposition. J Compos Mater 2021;55(26):3893–908.
[26] Reyes C, Somogyi R, Niu S, Cruz MA, Yang F, Catenacci MJ, Rhodes CP, Wiley BJ. Three-Dimensional printing of a complete lithium ion battery with fused filament fabrication. ACS Appl Energy Mater 2018;1(10):5268–79.
[27] Galos J, Pattarakunnan K, Best AS, Kyratzis IL, Wang C-H, Mouritz AP. Energy storage structural composites with integrated lithium-ion batteries: a review. Adv Mater Technol 2021:2001059. **n/a**(n/a).
[28] Fredi G, Jeschke S, Boulaoued A, Wallenstein J, Rashidi M, Liu F, Harnden R, Zenkert D, Hagberg J, Lindbergh G, Johansson P, Stievano L, Asp LE. Graphitic microstructure and performance of carbon fibre Li-ion structural battery electrodes. Multifunct Mater 2018;1(1):015003.
[29] Sharma M, Gao S, Mäder E, Sharma H, Wei LY, Bijwe J. Carbon fiber surfaces and composite interphases. Compos Sci Technol 2014;102:35–50.
[30] Pérez-Pacheco E, Cauich-Cupul JI, Valadez-González A, Herrera-Franco PJ. Effect of moisture absorption on the mechanical behavior of carbon fiber/epoxy matrix composites. J Mater Sci 2013;48(5):1873–82.
[31] Chen Q, Xu R, He Z, Zhao K, Pan L. Printing 3D gel polymer electrolyte in lithium-ion microbattery using stereolithography. J Electrochem Soc 2017;164(9):A1852–7.
[32] Gabriel S, Jérôme R, Jérôme C. Cathodic electrografting of acrylics: from fundamentals to functional coatings. Prog Polym Sci 2010;35(1):113–40.
[33] Thorat IV, Mathur V, Harb JN, Wheeler DR. Performance of carbon-fiber-containing LiFePO4 cathodes for high-power applications. J Power Sources 2006;162(1):673–8.
[34] Hu Y, Doeff MM, Kostecki R, Fiñones R. Electrochemical performance of sol-gel synthesized LiFePO[sub 4] in lithium batteries. J Electrochem Soc 2004;151(8):A1279.
[35] Guoping W, Qingtang Z, Zuolong Y, MeiZheng Q. The effect of different kinds of nano-carbon conductive additives in lithium ion batteries on the resistance and electrochemical behavior of the LiCoO2 composite cathodes. Solid State Ionics 2008;179(7):263–8.
[36] Dong G-H, Mao Y-Q, Wang D-Y, Li Y-Q, Song S-F, Xu C-H, Huang P, Hu N, Fu S-Y. Lithium metal structural battery developed with vacuum bagging. J Mater Chem C 2022;10(5):1887–95.
[37] Ihrner N, Johannisson W, Sieland F, Zenkert D, Johansson M. Structural lithium ion battery electrolytes via reaction induced phase-separation. J Mater Chem 2017;5(48):25652–9.
[38] Font F, Protas B, Richardson G, Foster JM. Binder migration during drying of lithium-ion battery electrodes: modelling and comparison to experiment. J Power Sources 2018;393:177–85.
[39] Postiglione G, Natale G, Griffini G, Levi M, Turri S. Conductive 3D microstructures by direct 3D printing of polymer/carbon nanotube nanocomposites via liquid deposition modeling. Compos Appl Sci Manuf 2015;76:110–4.
[40] Bruneaux J, Therriault D, Heuzey M-C. Micro-extrusion of organic inks for direct-write assembly. J Micromech Microeng 2008;18(11):115020.
[41] Kalnaus S, Asp LE, Li J, Veith GM, Nanda J, Daniel C, Chen XC, Westover A, Dudney NJ. Multifunctional approaches for safe structural batteries. J Energy Storage 2021;40:102747.